ORIGINAL ARTICLE

A triple-coil electromagnetic two-step forming method for tube fitting

Qi Xiong [1,2] · Xiang Zhao [1,2] · Hang Zhou [1,2] · Meng Yang [3] · Lijun Zhou [1,2] · Dun Gao [1,2] · Shengfei Li [1,2]

Abstract

Electromagnetic forming (EMF) is widely used in the processing of tube fittings in the fields of aerospace, automobile, and other industrial manufacturing because of its high energy rate, which can significantly improve the forming limit of light-weight metal materials. One typical application of EMF is the tube attraction by a double-coil electromagnetic single-step (DCSS) forming method. However, the electromagnetic force in this method is unevenly distributed on the tube, which will affect the uniformity of the final shape and undermine the performance of the workpiece. To solve this problem, a triple-coil two-step forming (TCTS) method is proposed in this paper. An electromagnetic-structure coupling finite element model is established to analyze the forming process in both DCSS and TCTS methods; the tube forming uniformity in both methods is compared. To quantify the uniformity of tube, the forming uniform length, $D_{uniform}$, is introduced and the area where the deformation is greater than 99% of the maximum deformation is defined as the forming uniform length. The simulation results show that when using the DCSS method, $D_{uniformD}$=3.73mm, and when using TCTS method, $D_{uniformT}$=11.63mm. The TCTS method increases the forming uniform length by 211%. All these results indicate the potential and the prospect of TCTS method for improving the forming uniformity of tube fittings.

Keywords Aluminum alloy · Electromagnetic forming · TCTS method · Tube bulging · Tube forming uniformity

1 Introduction

Electromagnetic forming (EMF) is a high-energy and high-speed processing method which uses coils to generate pulse Lorentz force in the metal workpiece to achieve plastic deformation [1]. Electromagnetic expansion is one of the most effective approaches to expand the aluminum alloys tube. Compared with traditional bulging technology, electromagnetic bulging has a lot of advantages like good controllability, high machining efficiency, and large forming limit [2].

At present, there are two forms of electromagnetic bulging. The first one, as shown in Fig. 1a, is electromagnetic bulging based on repulsive force [3]. A coil carrying a pulse current is placed inside the tube. The coil generates a high pulse magnetic field and then an eddy current is induced in the tube. The eddy current and magnetic field can generate a huge repulsive force to drive the tube bulge. The second one, as shown in Fig. 1b, shows an opposite way to achieve electromagnetic bulging by an attraction force [4, 5]. In this method, two coils are placed outside the tube. Two power supplies are used to drive the coils. One passes a long pulse current to the outer coil to provide a background magnetic field. The other passes a short pulse current to the inner coil to generate eddy current in the tube. By elaborate design of the two power supplies, an attraction force can be generated to drive the bulging of the tube. Li et al. designed the EMF system that can be applied to 1-mm-thick AA6061 tubes and prove its effectiveness by both simulations and experiments [6]. Xiong et al. conducted a series of studies on the electromagnetic forming process of attraction [7, 8]. However, no matter it is repulsive or attractive, there is a problem of poor bulging uniformity in both methods. Repulsive electromagnetic bulging can improve the

✉ Qi Xiong
pandaqi0218@gmail.com

1 College of Electrical Engineering & New Energy, China Three Gorges University, Yichang 443002, China

2 Hubei Provincial Engineering Technology Research Center for Power Transmission Line, China Three Gorges University, Yichang 443002, China

3 Suixi Power Supply Company, State Grid Anhui Electric Power Co. Ltd., Huaibei 235100, China
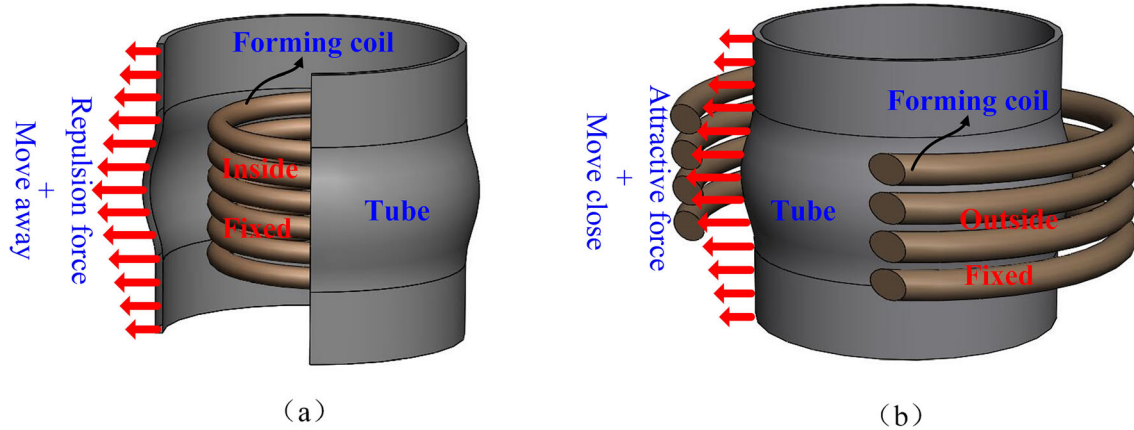
Fig. 1 Schematic diagram of tube bulging. **a** Repulsive electromagnetic bulginga. **b** Attractive electromagnetic bulging [4]

uniformity of bulging by adding a mold on the outside of the tube. Yu et al. analyzed the electromagnetic calibration process of pipe fittings, conducted experimental research on the calibration process, and used molds to perform uniformity calibration on the tube fitting ports [9]. Yu et al. used a mold to uniformly shape a 5A20 round aluminum tube into a square tube [10]. Ouyang et al. used a three-coil repulsion electromagnetic forming system to optimize the electromagnetic force distribution and improve the uniformity of the tube forming [11]. But it is difficult to do so in an attractive method due to the space limitation between the coil and the tube. This also greatly increases the difficulty of improving the uniformity of the tube bulging.

To solve these above problems, a triple-coil two-step forming system is presented, in which three coils are placed on the outside of the tube. The system consists of three sets of power systems and three sets of coils, through precise control of the discharge current and the timing coordination of the three sets of power discharges to achieve the TCTS method, improve the uniformity of attracting electromagnetic bulging. To verify the effectiveness of the method, the principle of the TCTS method was analyzed theoretically at first. Then, an electromagnetic-structure coupling model was built for simulation, and credible results were obtained.

2 Basic principles of TCTS method

In the process of electromagnetic forming, it can be obtained from Maxwell's equations

$$\nabla \times E_\varnothing = -\frac{\partial B}{\partial t} + \nabla \times (v \times B) \tag{1}$$

where $E_\varnothing$ is the circumferential electric field strength, B is magnetic field intensity, $\frac{\partial B}{\partial t}$ is the induced electromotive force, v is the workpiece speed, and $\nabla \times (v \times B)$ is the motional electromotive force. There are also:

$$J_\varnothing = \gamma E_\varnothing \tag{2}$$

where $J_\varnothing$ is the density of circumferential eddy current, and γ is the conductivity of the tube. Equations (1) and (2) show the cause of the induced eddy current in the tube during EMF.

The interaction between the induced eddy current in the tube fittings and space magnetic field will generate Lorentz force. According to the expression of Lorentz force:

$$f = J_\varnothing \times B \tag{3}$$

where f is Lorentz force. Then, the Lorentz force is divided into two parts: radial and axial [8]

$$f_r = J_\varnothing \times B_z \tag{4}$$

$$f_z = -J_\varnothing \times B_r \tag{5}$$

where f_r and f_z are radial Lorentz forces and axial Lorentz forces. B_r and B_z are the axial components and the radial
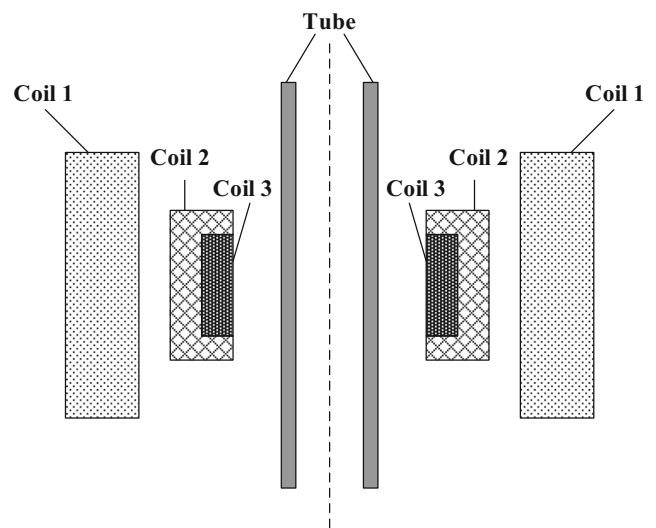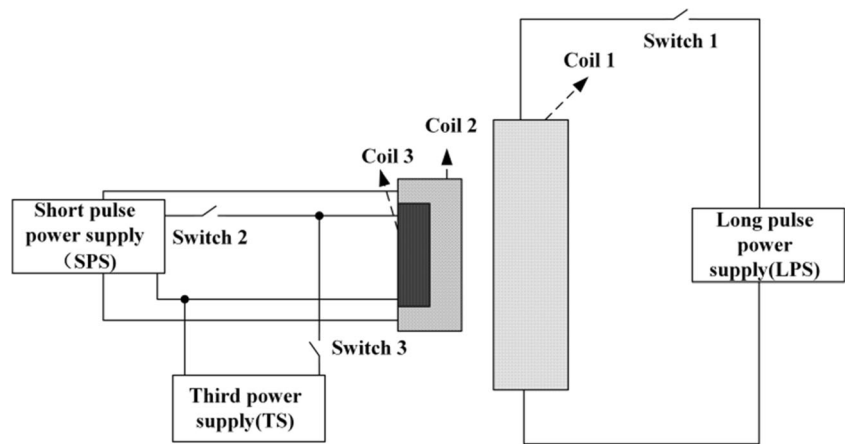

Fig. 2 Schematic of electromagnetic bulging system

Fig. 3 Coil current loading system

component of the magnetic flux density respectively.

Fig. 2 shows the electromagnetic bulging system used in this article. Fig. 3 shows the coil current loading system.

Fig. 4 shows the power loading sequence. The long pulse power supplies (LPS) a long pulse current i_{cl} to coil 1, reaching the peak value at t_1, the short pulse power supplies (SPS) a short pulse current i_{cs} to coil 2 and coil 3. They are running in parallel. The tube is bulged by attraction which arises at t_1 and ends at t_2. After t_2, the SPS stops supplying power to coil 3, and the third power supply (TS) starts supplying current i_{cT} flows into coil 3.

So radial Lorentz force density in Eq. (4) can be replaced by:

$$f_r = \begin{cases} J_{\varnothing-l} \times (-B_{Z-l}), (t < t_1) \\ -(J_{\varnothing-s}-J_{\varnothing-l}) \times (-B_{Z-l} + B_{Z-s}), (t_1 \le t < t_2) \\ J_{\varnothing-T} \times (-B_{Z-T}), (t \ge t_2) \end{cases} \quad (6)$$

where $J_{\varnothing-l}$, $J_{\varnothing-s}$, and $J_{\varnothing-T}$ are the eddy current densities caused by the short pulse current, the long pulse current, and the current of the TS. B_{Z-l}, B_{Z-s}, and B_{Z-T} are the axial magnetic fields generated by the long pulse current, the short pulse current, and the current of TS.

3 Simulations

At present, many simulation models were established, and Li et al. wrote a set of algorithms and successfully realized electromagnetic forming simulation using finite element software [12, 13]. Cao et al. used COMSOL to establish a set of algorithms to simulate the electromagnetic forming process [14]. This part uses COMSOL to establish a two-dimensional axisymmetric bidirectional coupling model, and its algorithm flow is shown in Fig. 5 [14]. This simulation method has been widely used in electromagnetic forming [15, 16].
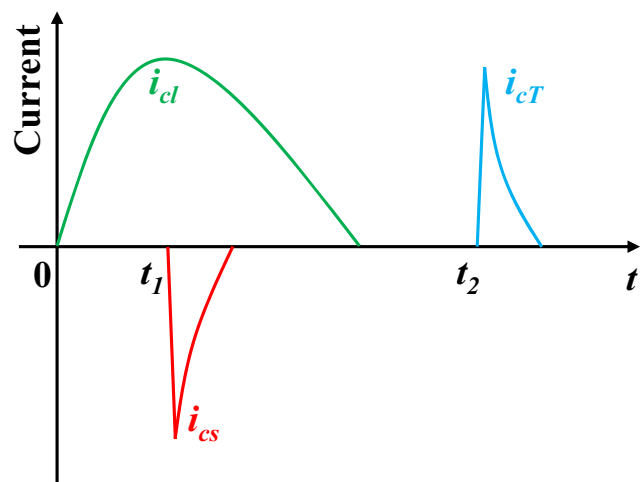
3.1 Circuits

According to the principle described above, its specific circuit model as shown in Fig. 6, the three sets of power supply are controlled by computer, and the TCTS method processing is completed with precise cooperation. And their parameters are shown in Table 1.

3.2 Coil

The electromagnetic field model consists of three coils and one tube, and its spatial distribution is shown in Fig. 7.

3.3 Material

On the basis of the engineering material characteristics database (https://www.makeitfrom.com/material-properties/6063-T83-Aluminum), this paper did a tensile experiment on A6063-T83 aluminum alloy and obtained the real parameters of the tube. These simulations used AA6063-T83 tube fittings with a height of 90mm, a thickness of 1mm, and an inner

Fig. 4 Timing diagram of power loading

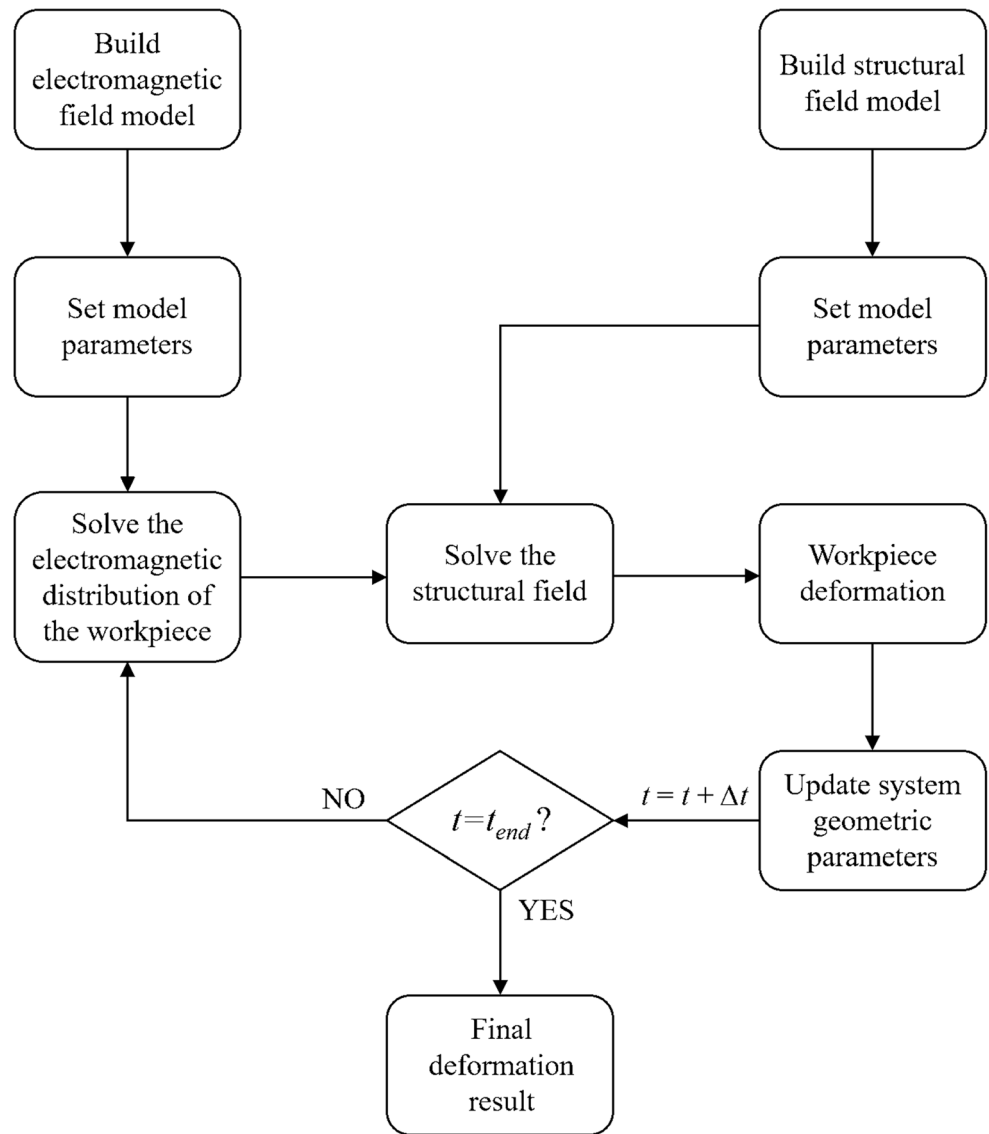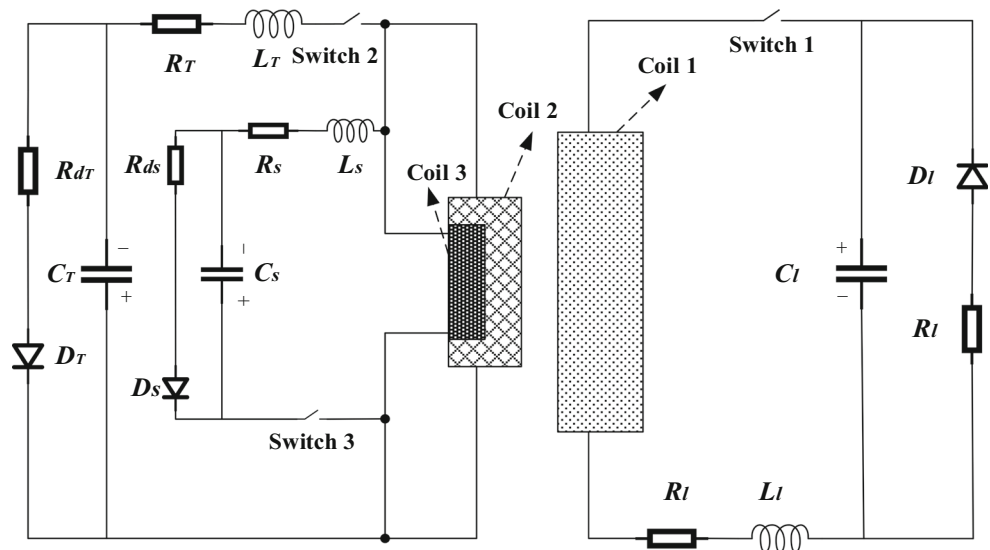**Fig. 5** Flowchart of the
implemented algorithm

Fig. 6 Circuit model

Table 1 Circuit parameters

Discharge parameters	Short pulse power supply (SPS)		Long pulse power supply (LPS)		Third power supply (TS)	
	Symbol	Value	Symbol	Value	Symbol	Value
Initial discharge voltage	U_s	5.5kV	U_l	3.8kV	U_T	7kV
Capacitance	C_s	320uF	C_l	2880uF	C_T	290uF
Line resistance	R_s	8mΩ	R_l	15mΩ	R_T	7mΩ
Line inductance	L_s	20uF	L_l	4uF	L_T	20uF
Crowbar resistance	R_{ds}	10mΩ	R_{dl}	100mΩ	R_{dT}	10mΩ

radius of 20mm. Its elastic modulus was 69 GPa, the Poisson ratio was 0.33, and the initial yield tensile strength was 230 MPa. In the electromagnetic forming process, the workpiece moves very quickly, so the stress-strain relationship has a powerful influence on the deformation of the workpiece. Therefore, the Cowper-Symonds constitutive model is used to analyze the deformation of the tube [17]. The model is as follows:

$$\sigma = \sigma_y \left[1 + \left(\frac{\varepsilon}{C} \right)^m \right] \tag{7}$$

where σ_y and ε are yield stress (MPa) and the plastic strain rate (s^{-1}) respectively. For aluminum alloy, $C = 6500\ s^{-1}$, $m = 0.25$.
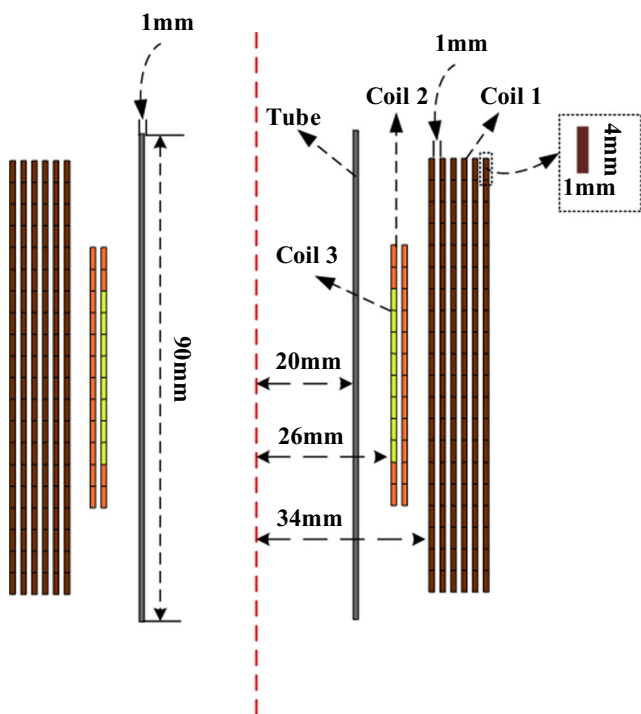

Fig. 7 Electromagnetic field geometry model

4 Results and discussion

## 4.1 The influence of TCTS method on tube bulging uniformity

In the DCSS method, because of the uneven distribution of the radial electromagnetic force, the deformation of the tube is uneven. Moreover, due to the space limitation between the tube and the coil, it is difficult for the DCSS method to improve the uniformity of deformation by placing the mold. TCTS method can perform secondary processing on the unevenly deformed length after the attraction bulging is completed, and theoretically can improve the uniformity of the tube bulging. To study the effect of the TCTS method on the uniformity of the tube bulging, the results of the TCTS method with the results of the DCSS method under the same parameters are compared.

Fig. 8 shows the radial displacement of the outside of the tube under the two processing methods. It can be seen that the TCTS method makes the most unevenly bulging length of the tube fittings a flat top.
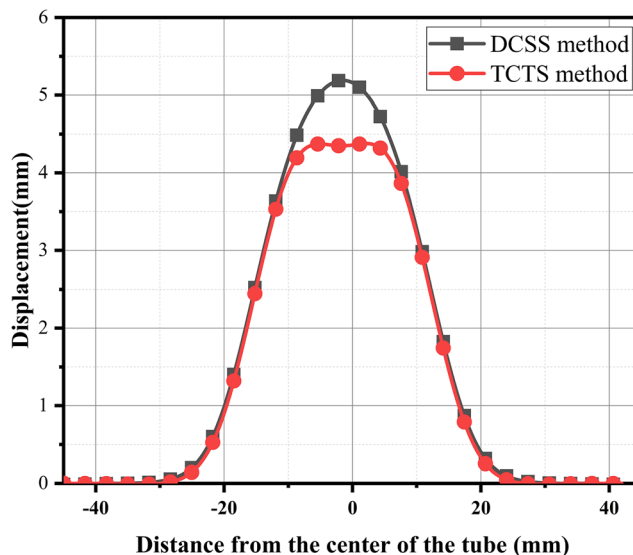
Fig. 8 The radial displacement of the outside of the tube under the two processing methods
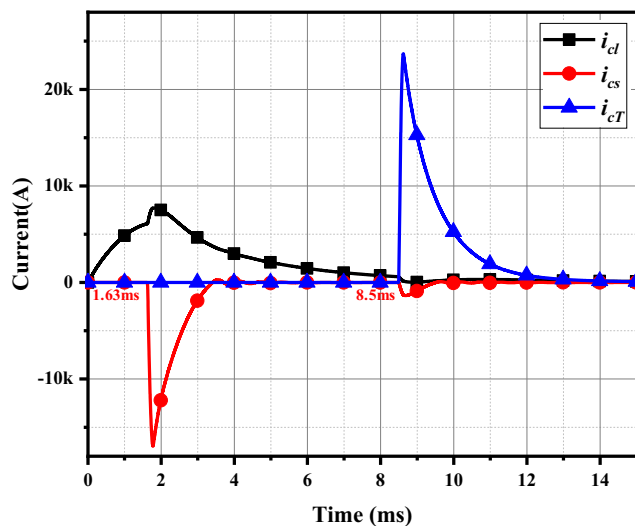
Fig. 9 Tube forming contours in two forming methods. **a** DCSS method. **b** TCTS method
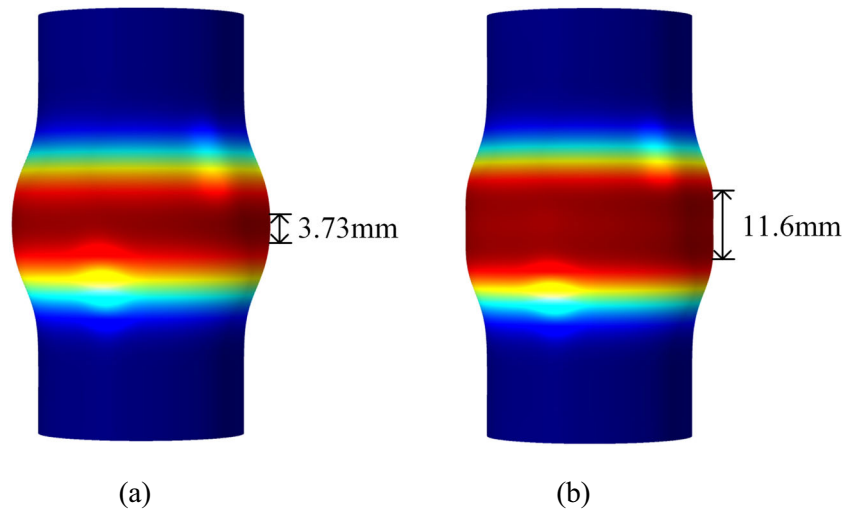
(a)   (b)

To quantify the effect of the TCTS method on the uniformity of the tube, the forming uniform length $D_{uniform}$ is introduced, and the area where the deformation is greater than 99% of the maximum deformation is defined as the forming uniform length $D_{uniform}$. As shown in Fig. 9, the simulation results show that when using the DCSS method, $D_{uniformD}$=3.73mm, and when using the TCTS method, $D_{uniformT}$=11.63mm. The TCTS method increases the forming uniform length by 211%. Obviously, the TCTS method can effectively improve the uniformity of tube fittings. Next, the deformation process of the tube will be analyzed.

4.2 TCT method process

Fig. 10 shows the current timing diagram of the three coils. First, LPS supplies a long pulse current i_{cl} to coil 1, which reaches the peak value at t=1.63ms. At t=1.63ms, SPS supplies a short pulse current i_{cs} to coil 2 and coil 3. They are running in parallel. The tube is bulged by attraction force since

t=1.63ms and the attraction force ends at t=8.5ms. After t=8.5ms, the SPS stops supplying power to coil 3, and the TS starts supplying. This is the timing coordination scheme of the three groups of power supplies. Fig. 11 reflects the distribution of Lorentz force in the TCTS method process. The results show that: (1) Lorentz force reverses at i_{cl} loading time (1.64ms) and i_{cT} loading time (8.51ms). (2) The first reversal of the Lorentz force causes the tube to bulge under the attraction force, and the second reversal causes the most unevenly deformed area of the tube to receive an inward repulsive force. This TCTS method format matches the design.

To better study the process of tube deformation, the movement process of point A in Fig. 11 is analyzed in detail here (point A is the midpoint of the tube). The axial magnetic field and the induced eddy current at point A are shown in Fig. 12. It can be seen that when t=1.63ms, the magnetic field

Fig. 10 Current timing coordination
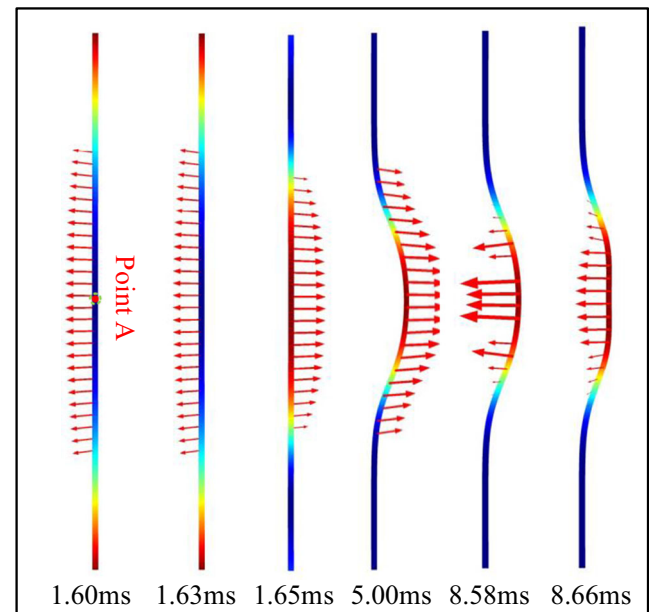
Fig. 11 The distribution of Lorentz force in the TCTS method

generated by the coil 1 reaches the peak value, and the short pulse width current passes into the coil 2 and the coil 3. They run in parallel. As a result, starting from t=1.63ms, the tube is subjected to a huge outward radial Lorentz force, and the tube is bulged by the attractive force. When t=8.5ms, the magnetic field generated by coil 1 is basically 0, and the TS supplies current passes into coil 3. The magnetic field generated by this current interacts with the eddy current, and the most uneven area of the tube bulging is affected by an inward radial Lorentz force.

Fig. 13 shows the radial electromagnetic force and displacement at point A. It can be seen that the radial electromagnetic force is negative when t<1.63ms, and the tube is driven by the electromagnetic force to make a small inward displacement. When t>1.63ms, the radial electromagnetic force suddenly increases in the reverse direction, and the tube begins to bulge under the attraction force. When t>8.5ms, the radial electromagnetic force is reversed again, and the most uneven area of tube bulging is displaced inward. The final radial displacement at point A is 4.4mm.

4.3 The influence of TS voltage U_T

The analysis above showed that the TCTS method is mainly composed of two parts: attraction and repulsion. When the parameters of the attraction force remain unchanged, the parameters of the TS will have a greater impact on the forming effect. This part analyzes the influence of the TS's parameters on the forming effect. With other parameters unchanged, a series of simulations were performed on different voltages U_T.

Fig. 14a shows the radial displacement of point A under different voltages. Since the parameters of the LPS and the SPS have not changed, there is no difference in the displacement of point A in the attraction phase, only the difference in the repulsive force phase. Moreover, the displacement of point A by the repulsive force is proportional to the magnitude of the voltage. When U_T=6kV, there is no displacement. This shows that the repulsive force generated when the voltage is too small is not enough to drive the deformation of the tube. Fig. 14b shows the tube deformation under different voltages. Table 2 shows the form uniform length $D_{uniform}$ under different voltage.

When the voltage is small, the displacement is not enough to make the tube uniform. However, the higher voltage is not better. The middle part of the tube will be excessively deformed. It can be seen that the displacement of the point A of the tube is much smaller than the maximum displacement when U_T=7.5kV and U_T=8kV, which will also cause uneven deformation of the tube. In this simulation, to make the tube more uniform, the final selected voltage value is 7kV. Although the maximum displacement is reduced, the reduced
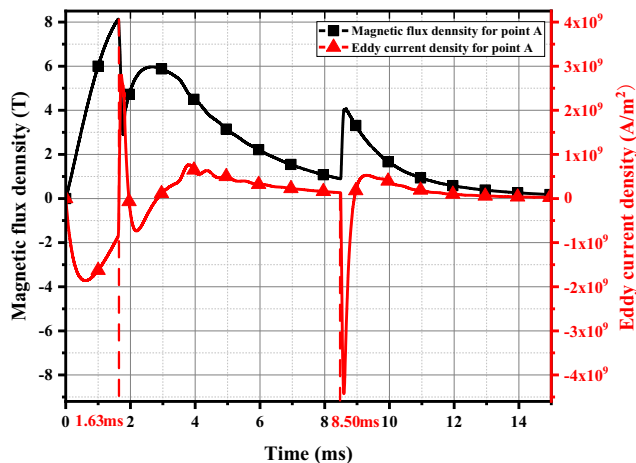

Fig. 12 The axial magnetic field and the induced eddy current at point A

length is the unevenly deformed length, which is exactly the length we hope to improve.

4.4 The influence of tube thickness on forming effect

Furthermore, the influence of tube thickness on the forming effect is studied. Different thicknesses of tube fittings have different forming effects under the same power supply parameter. This research can provide a basis for the optimization of power supply parameters by observing the forming effect of each tube.

Fig. 15a shows the radial displacement of point A under different tube thicknesses. The greater the thickness of the tube, the smaller the radial displacement. When the thickness of the tube is 1.1mm, the secondary processing has almost no effect on the uniformity of the tube.

Fig. 15b shows the outer displacement of the tube under different tube thicknesses. Combined with Table 3 Form uniform length $D_{uniform}$ under different tube thickness, when this set of parameters is applied to a thicker tube, although it can successfully make the tube bulge with the attractive force, it
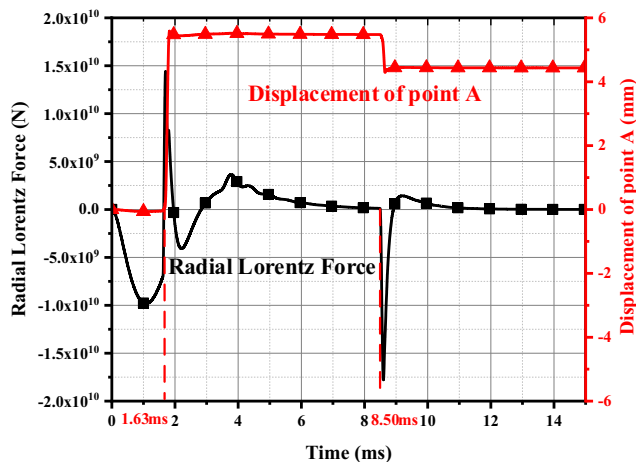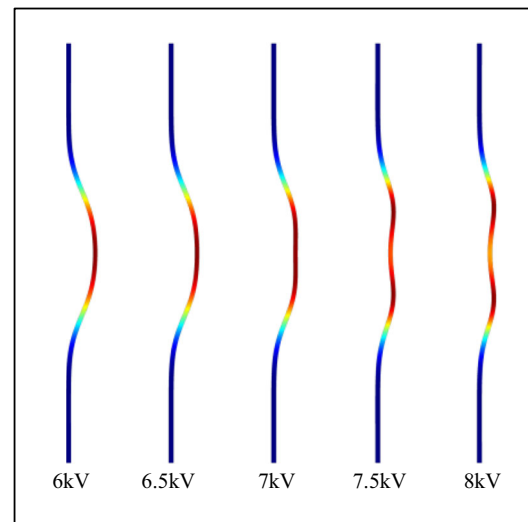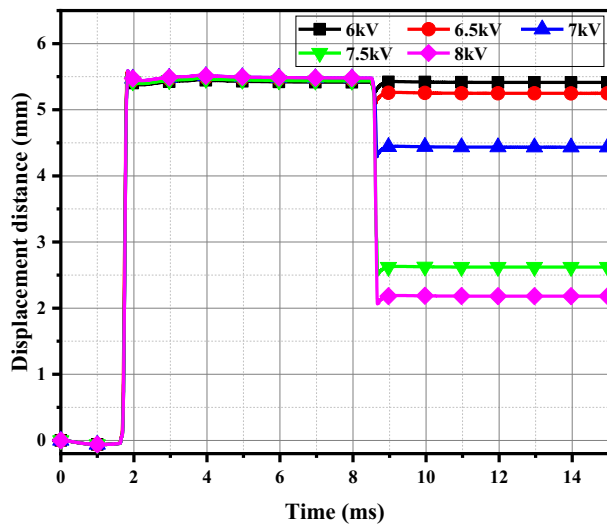

**Fig. 13** The radial electromagnetic force and displacement at point A

(a) Displacement of point A under different voltages　　(b) Tube deformation under different voltage

Fig. 14 Deformation behavior under different TS voltage U_T. **a** Displacement of point A under different voltages. **b** Tube deformation under different voltage

Table 2　The forming uniform length $D_{uniform}$ under different TS voltage U_T

TS voltage U_T (kV)	6	6.5	7	7.5	8
Displacement of point A (mm)	5.35	5.19	4.36	2.61	2.17
Maximum displacement (mm)	5.35	5.19	4.38	3.19	2.96
Form uniform length $D_{uniform}$ (mm)	3.92	4.80	11.63	3.40	3.20
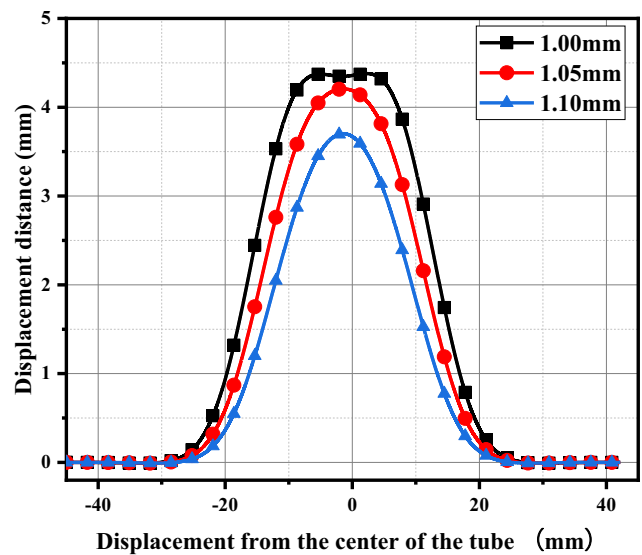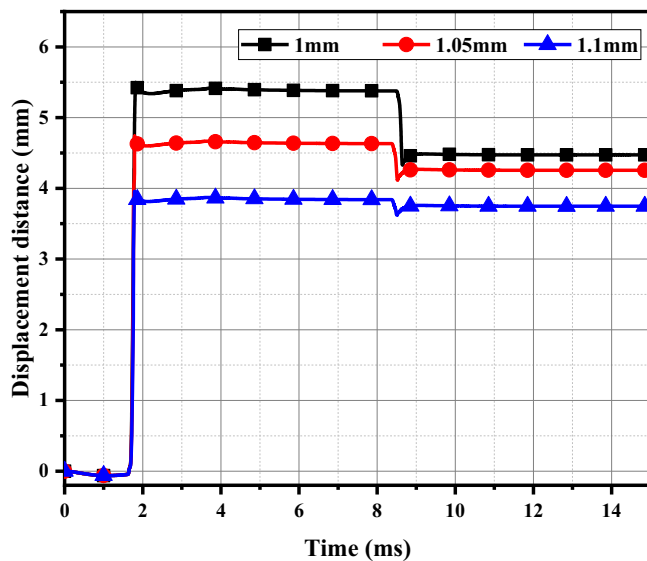
(a)　Displacement of point A　　　　　(b)　Outer displacement of the tube

Fig. 15 Deformation behavior under different tube thickness. **a** Displacement of point A. **b** Outer displacement of the tube

**Table 3** Form uniform length $D_{uniform}$ under different tube thickness

Tube thickness (mm)	1	1.05	1.10
Displacement of point A (mm)	4.36	4.20	3.70
Maximum displacement (mm)	4.38	4.20	3.70
Form uniform length $D_{uniform}$ (mm)	11.63	3.78	3.00

does not produce a better uniform effect. This is closely related to the force of the tube fittings. As shown in Fig. 16, the secondary processing radial Lorentz force under different tube thicknesses is analyzed.

The greater the thickness of the tube is, the smaller the radial Lorentz force is. Because when the thickness of the tube becomes larger, the bulging depth in the tube due to the attractive force of the first step processing will become smaller, and the distance between the coil and the tube will be larger in the secondary processing. Therefore, the radial Lorentz force received by the tube becomes decreases. But it does not mean that this system is not suitable for the tube with higher thickness. It only needs to adjust some power parameters to improve the forming effect.

To improve the forming effect of the tube fittings, it is necessary to increase the attractive force to increase the bulging depth of the attractive force. To make the tube bulge uniform, when the thickness of the tube increases, the power energy of the secondary processing also needs to increase. According to the previous analysis, increasing the voltage of the TS can increase the powerful energy in the secondary processing. Take the tube with a thickness of 1.1mm as an example to optimize the power supply parameters, and the optimized parameters are shown in Table 4.

The attractive force is increased by increasing the voltage of LPS and TPS. The energy of secondary processing is
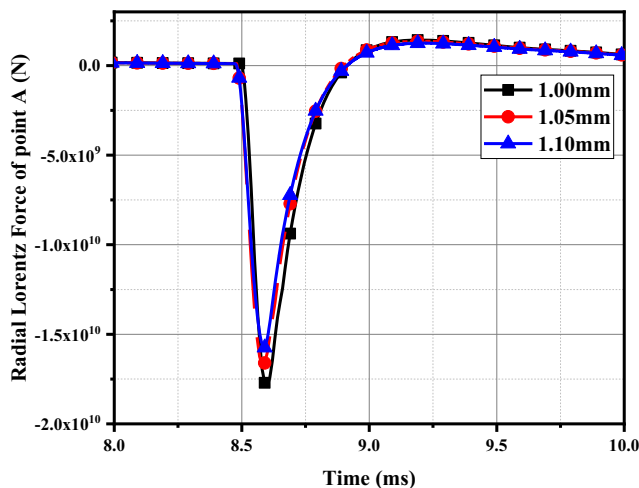

Fig. 16 The secondary processing radial Lorentz force under different tube thicknesses

Table 4 The optimized circuit parameters

Discharge parameters	Short pulse power supply (SPS)		Long pulse power supply (LPS)		Third power supply (TS)	
	Symbol	Value	Symbol	Value	Symbol	Value
Initial discharge voltage	U_s	6kV	U_l	4kV	U_T	7.3kV
Capacitance	C_s	320uF	C_l	2880uF	C_T	290uF
Line resistance	R_s	8mΩ	R_l	15mΩ	R_T	7mΩ
Line inductance	L_s	20uF	L_l	4uF	L_T	20uF
Crowbar resistance	R_{ds}	10mΩ	R_{dl}	100mΩ	R_{dT}	10mΩ

Fig. 17 Comparison of forming effect before and after optimization

(a) Before optimization   (b) After optimization
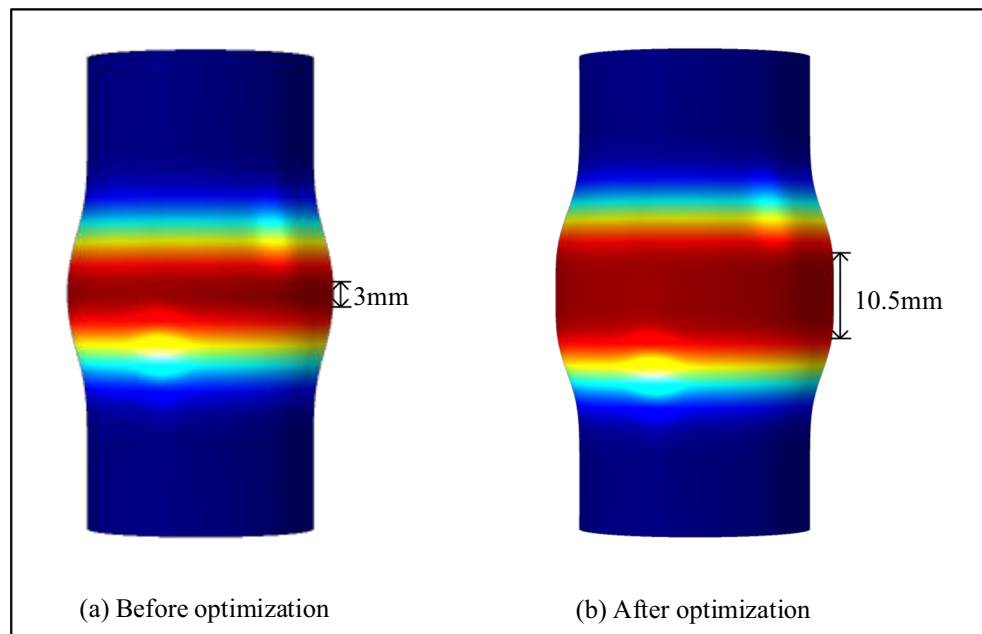
increased by the TS voltage. Fig. 17 shows the comparison of forming effects. The simulation results show that when the parameters are optimized, $D_{uniformO}$=10.50mm. The form uniform length after optimizing the parameters is 250% higher than before. This also shows that the TCTS method can be used in tubes of various thicknesses.

5 Conclusions

To improve the forming uniformity of tube fittings, a TCTS method system is presented, in which three coils are placed on the outside of the tube. To quantify the effect of the TCTS method on the uniformity of the tube, the forming uniform length $D_{uniform}$ is introduced, and the area where the deformation is greater than 99% of the maximum deformation is defined as the forming uniform length. The simulation results show that when using the DCSS method, $D_{uniformD}$=3.73mm, and when using TCTS method, $D_{uniformT}$=11.63mm. The TCTS method increases the forming uniform length by 211%. Both theories and simulations show that through the timing coordination of the three sets of power supplies, the TCTS method can be realized and the uniformity of tube fittings can be improved. This method contributes to the expansion of electromagnetic forming. Then, the influence of tube thickness on the forming effect is studied. And, methods to improve the forming quality of tube fittings have been verified for different tube thicknesses.

Author contribution Qi Xiong: conceptualization, methodology, formal analysis, writing

Xiang Zhao: methodology, software, investigation, writing–original draft

Hang Zhou: writing–original draft

Meng Yang: software, methodology, visualization

Lijun Zhou: software

Dun Gao: investigation

Shengfei Li: formal analysis

Data availability All the data have been presented in the manuscript.

Declarations

Conflict of interest The authors declare no competing interests.

References

1. Psyk V, Risch D, Kinsey BL, Tekkaya AE, Kleiner M (2011) Electromagnetic forming—a review. J Mater Process Technol 211(5):787–829

2. Xiong Q, Tang H, Wang M, Huang H, Jiang J, Qiu L (2019) Research progress of electromagnetic forming technique since 2011. High Voltage Eng 45(4):1171–1181

3. Xiong Q, Tang H, Wang M, Huang H, Qiu L, Yu K, Chen Q (2019) Design and implementation of tube bulging by an attractive electromagnetic force. J Mater Process Technol 273:116240

4. Li X, Cao Q, Lai Z, Ouyang S, Liu N, Li M, Li L (2020) Bulging behavior of metallic tubes during the electromagnetic forming process in the presence of a background magnetic field. J Mater Process Technol 276:116411

5. Zhang X, Ouyang S, Li X, Li L, Deng F (2020) Effect of pulse width of middle-coil current on deformation behavior in electromagnetic tube forming under two-stage coils system. Int J Adv Manuf Technol 110(5):1139–1152

6. Ouyang S, Li X, Li C, Du L, Peng T, Han X, Cao Q (2020) Investigation of the electromagnetic attractive forming utilizing a dual-coil system for tube bulging. J Manuf Process 49:102–115

7. Xiong Q, Yang M, Liu X, Song X, Qiu L, Jiang J, Yu K (2020) A dual-coil method for electromagnetic attraction forming of sheet metals. IEEE Access 8:92708–92717

8. Xiong Q, Yang M, Tang H, Huang H, Song X, Qiu L, Cao Q (2020) Flaring forming of small tube based on electromagnetic attraction. IEEE Access 8:104753–104761

9. Yu Y, Li C, Jiang H, Yu H (2005) Experimental study of tube ends sizing with electromagnetic bulging. Forging Stamping Technol 030(004):9–12. https://doi.org/10.3969/j.issn.1000-3940.2005.04.004

10. Yu H, Chen J, Liu W, Yin H, Li C (2018) Electromagnetic forming of aluminum circular tubes into square tubes: experiment and numerical simulation. J Manuf Process 31:613–623

11. Ouyang S, Wang C, Li C, Li X, Lai Z, Peng T, Li L (2021) Improving the uniformity and controllability of tube deformation via a three-coil forming system. Int J Adv Manuf Technol 114(5):1533–1544

12. Feng H, Cui X, Li G (2017) Coupled-field simulation of electromagnetic tube forming process using a stable nodal integration method. Int J Mech Sci 128:332–344

13. Li S, Cui X, Li G (2017) Multi-physics analysis of electromagnetic forming process using an edge-based smoothed finite element method. Int J Mech Sci 134:244–252

14. Cao Q, Li L, Lai Z, Zhou Z, Xiong Q, Zhang X, Han X (2014) Dynamic analysis of electromagnetic sheet metal forming process using finite element method. Int J Adv Manuf Technol 74(1-4):361–368

15. Yang M, Yan J, Song X, Qiu L, Jiang J, Yu K, Khan CA (2020) Optimization of the attractive electromagnetic bulging of small tubes based on non-uniform solenoid coils. IEEE Access 8:113121–113130

16. Xiong Q, Tang H, Deng C, Li L, Qiu L (2017) Electromagnetic attraction-based bulge forming in small tubes: fundamentals and simulations. IEEE Trans Appl Supercond 28(3):1–5

17. Xiong Q, Huang H, Xia L, Tang H, Qiu L (2019) A research based on advance dual-coil electromagnetic forming method on flanging of small-size tubes. Int J Adv Manuf Technol 102(9):4087–4094